Thin Solid Films 607 (2016) 67–72

Contents lists available at ScienceDirect

Thin Solid Films

journal homepage: www.elsevier.com/locate/tsf

Effect of metal doping on structural characteristics of amorphous carbon system: A first-principles study

Xiaowei Li [a], Dong Zhang [a], Kwang-Ryeol Lee [b], Aiying Wang [a]

[a] Key Laboratory of Marine Materials and Related Technologies, Key Laboratory of Marine Materials and Protective Technologies of Zhejiang Province, Ningbo Institute of Materials Technology and Engineering, Chinese Academy of Sciences, Ningbo 315201, PR China
[b] Computational Science Center, Korea Institute of Science and Technology, Seoul 136-791, South Korea

ARTICLE INFO

Article history:
Received 7 April 2015
Received in revised form 1 April 2016
Accepted 2 April 2016
Available online 7 April 2016

Keywords:
Transition metals
Amorphous carbon
Bonding
Residual stress
First-principles calculation

ABSTRACT

First-principles calculation was performed to investigate the effect of metal doping on the structural characteristics of amorphous carbon system, and the 3*d* transition metals (TM) were particularly selected as representative case. Results showed that the total energy in TM–C systems caused by distorting the bond angles was reduced distinctly for comparison with that in C–C system. Further electronic structure revealed that as the 3*d* electrons of doped TM increased, the bond characteristic of highest occupied molecular orbital changed from bonding (Sc, Ti) to nonbonding (V, Cr, Mn, Fe) and finally to antibonding (Co, Ni, Cu) between the TM and C atoms. Meanwhile, the TM–C bond presented a mixture of the covalent and ionic characters. The decrease of strength and directionality of TM–C bonds resulted in the total energy change upon bond angle distortion, which demonstrated that the bond characteristics played an important role in reducing residual stress of TM-doped amorphous carbon systems.

1. Introduction

Diamond-like carbon films (DLC) have attracted extensive interests from scientific disciplines and industrial societies due to their unique structures and excellent mechanical, electronic, optical as well as magnetic properties [1–4], which are widely used as protective coatings in the fields of automobile engine components, solar cells, data storages, biomedical implants, etc. [5–7]. More recently, from the technical performance, DLC films are functionalized by the addition of third transition metals (TM), such as Ti, W, Cr, Fe, Ni, Cu, and Ag, to overcome their high residual stress and improve other properties [8–13]. Note that, however, the strong dependence of structures on the variety and content of doped metal atoms and the diversity of deposition techniques lead to the disputable understanding for the effect of doped metal on the film structure and physical and chemical properties. In particular, the stress reduction mechanism of TM–C system caused by the metal doping is still in its infancy. For example, doping Ti, W, or Cr into amorphous carbon matrix decreased the stress without seriously deteriorating the hardness because of the partly formed hard carbide nano-particulates, increased sp^2 graphitization, C-sp^3 substitution by doped TM atoms as well as the proposed pivot relaxation role [8,14]. While the alloying of DLC with Cu, Ag or Al generally led to the formation of soft and ductile phase, and thus both the stress and hardness decreased significantly [15–17]. To distinctly address the reason for the reduced residual stress caused by the metal doping, understanding the structural characteristics of TM-doped amorphous carbon system from the atomic scale is necessary.

Recently, Wang et al. found that due to the reduced directionality of the W–C bonds, the doped W atoms could play a pivotal action to decrease the strain energy arising from the distortion of the bond angles, resulting in a significant reduction of residual stress [9]. Choi et al. [18] also performed the first-principles calculation using the same simplified tetrahedral model and revealed the bond characteristics of TM–C system by the doping of Mo, Ag, or Al, respectively, from which the effect of metallic impurities in carbon materials could be explained. Nevertheless, the previous works paid no attention to the strong correlation between the structural characteristics and the valence electrons of the doped TM atoms. A more systematic study of TM–sp^3–carbon interactions in TM–C system, such as their electronic structure and electron transfer behaviors, is needed to fully understand the general behavior of these TM–C structures and explore the dependence of bond characteristics on *d* electrons.

In this paper, the structural characteristics and bond interactions of TM–C system were investigated by the first-principles calculation. In order to elucidate the role of valence electrons on the bond structures, we selected all 3*d* TMs from Sc to Cu as the representative TM elements. It is well known that the mechanical properties of DLC films are related with the tetra-coordinated C atoms content, and the previous study also revealed the high residual stress mainly attributed to both the bond angle and bond length distortions [19], so the tetrahedral model was used for C(TM)–C systems, and the structural evolutions with the

E-mail addresses: krlee@kist.re.kr (K.-R. Lee), aywang@nimte.ac.cn (A. Wang).

http://dx.doi.org/10.1016/j.tsf.2016.04.004
0040-6090/

bond angles were evaluated by the partial density of states (PDOS), charge density distributions and molecular orbital (MO) diagrams. The obtained distinct changes in TM–C bond characteristics by comparing with that in C–C system were discussed to understand the general experimental phenomena, in which the significant reduction of residual stress was visible due to the doping of TM into amorphous carbon matrix.

2. Computational details

Fig. 1 shows the schematics of employed tetrahedral bond model, in which four carbon atoms are arranged as a tetrahedron with either a carbon or TM in the center and each peripheral carbon atom is terminated by hydrogen atoms for the sake of simplicity. This model had been proved to be satisfactory to provide a reasonable explanation for the experiments in amorphous carbon system [9,18]. All 3*d* TMs from Sc to Cu were selected particularly as the representative substitution of the central carbon atom in the tetrahedral TM-C system. The structure with a bond angle of 109.471° was chosen as a reference state (Fig. 1(a)). When the bond angle was distorted in a range of 90–130° (Fig. 1(b)), the structural relaxation could be characterized from the electronic structure and the change of total energy in TM–C system. Details of calculation model can be found in elsewhere [18], which has proved that this model is appropriate for investigating metal incorporation (or adsorption) into a carbon network even when the distorted structure is generated using a constrained relaxation.

All the spin-polarized first-principles calculations were performed by the DMol^3 software package (Accelrys Inc.) based on the density functional theory. The exchange-correlation was handled in the generalized gradient approximation with the Perdew–Burke–Ernzerhof parameterization [20], and all electrons double-numerical polarization basis was used. A self-consistent field was created using an energy convergence criterion of 10^{-5} eV, and atomic relaxation was repeated until the forces acting on the atoms were below 0.01 eV/Å. The Kohn–Sham wave functions were expanded to an orbital cutoff of 9 Å to guarantee convergence. A cubic supercell with a lateral size of 15 Å was used to avoid interactions between the adjacent images of the model.

3. Results and discussion

Fig. 2 shows the values of electron density, ρ_{max}, in the unit of electrons/Å^3 right before its isosurfaces between the central TM and the peripheral carbon atoms are spatially separated. For comparison, the characteristic of C–C system was also performed. The isosurfaces of

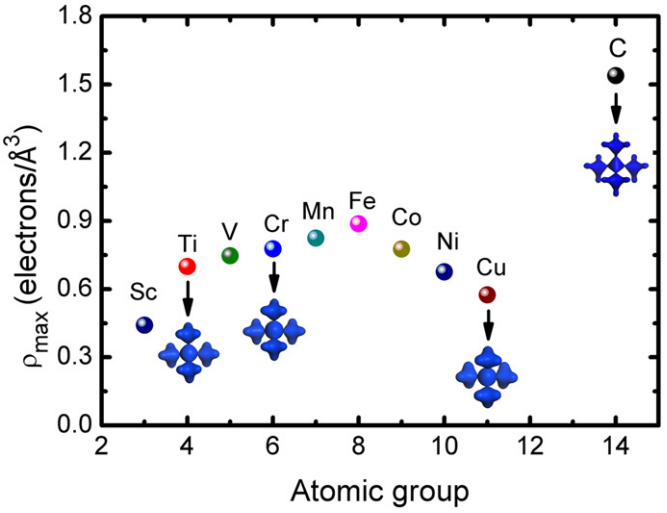

Fig. 2. Electron density before its isosurface is separated; the insets are the isosurfaces of electron density for C–C, Ti–C, Cr–C, and Cu–C systems right before the isosurfaces between the central atom and peripheral C atoms are separated.

electron density for C–C, Ti–C, Cr–C, and Cu–C systems are presented as insets of Fig.2, respectively. For C–C case, the maximal ρ_{max} of 1.5391 electrons/Å^3 and the strongest angular shape of isosurface imply the highest strength and directionality of C–C bonds. This is because the repulsive force between two carbon atoms can be counteracted by the higher electron density, which in turn drives the formation of more stable structure. On the contrary, when TM (Sc–Cu) replaces the central carbon atom in the unit, the ρ_{max} decreases significantly for each case following the increased isotropic characteristics of isosurface, indicating that both the strength and directionality of TM–C bonds are reduced. Since the structural distortion mainly arises from the distortion of both the bond angles and bond lengths, the different change of ρ_{max} with increasing the valence electrons of TMs may be one of the dominate factors for reducing the residual stress. Nevertheless, if one keeps in mind the disputed existence of stress reduction mechanism caused by various doped TM atoms in literatures [8–10, 14–17], as well as the changes, further insight into the bond characteristics and hybridization among atoms must be executed distinctly.

The bond characteristics in the system were analyzed using the PDOS for the model, the charge distribution of the highest occupied molecular orbital (HOMO) in the plane composed of the central atom and

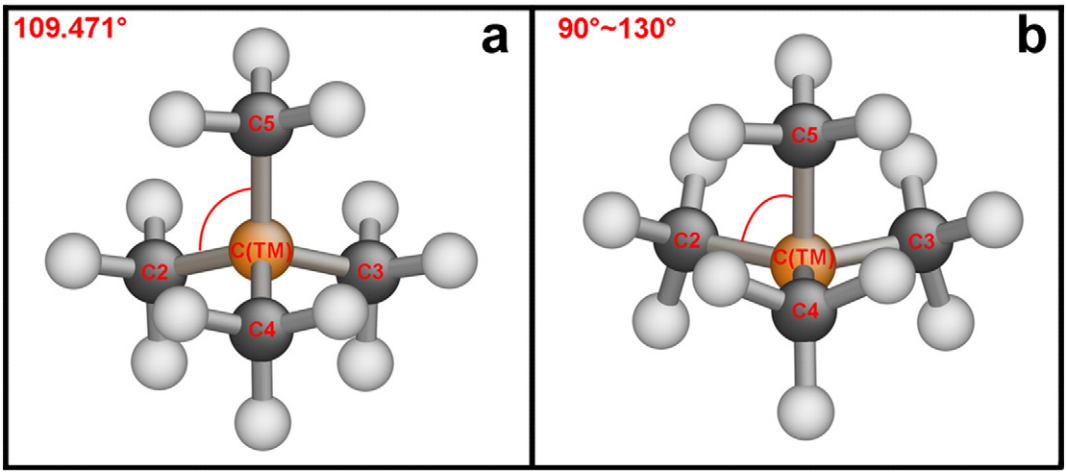

Fig. 1. (a) Reference state for the tetrahedral model with a carbon or TM atom (Sc–Cu) in the center with bond angles of 109.471°. (b) Distorted tetrahedral model where the three bond angles containing the central atom and peripheral carbon C5 were changed over the range from 90 to 130°. Black, yellow and white balls correspond to peripheral carbon, doped C(TM), and hydrogen atoms, respectively.

the peripheral carbon atoms, and the MO diagram. Figs. 3 and 4 show the spin resolved PDOS and spatial distribution of the charge density for the pure C–C, Ti–C, Cr–C, and Cu–C systems in the reference state, respectively. For the C–C system, the HOMO is strongly hybridized between the 2*p* orbitals of the carbon atoms, as shown in Fig. 3(a). In addition, the charge distribution of the HOMO (Fig. 4(a)) illustrates that the central carbon and peripheral carbon atoms are bonded with a heavy charge accumulation, which is the typical feature of the covalent bond with strong directionality. Fig. 5(a) shows the spin resolved MO diagrams of C–C system based on the PDOS calculation, in which the atomic orbitals were obtained from the electronic structure of the isolated atoms. The black and red arrows represent the spin down and spin up electrons, respectively. Based on the comparison between the energy levels for the HOMO and C 2*p* atomic state, the HOMO is proved to be a bonding state for C–C system and four electrons from the peripheral C 2*p* orbitals fill the bonding orbital in pairs combined with the electrons of the central C atoms, identifying the typical covalent bonding characteristic of C–C which should consequently strengthens the stability of the system.

With the addition of TM atom, it was found that the HOMO transitioned firstly from bonding state to nonbonding state, and then to antibonding state as the number of electrons in the 3*d* shell increased. Three representative cases for Ti, Cr, and Cu are presented in Fig. 3(b)–(d), Fig. 4(b)–4(d) and Fig. 5(b)-5(d). Fig. 3(b) shows the PDOS for the Ti–C system, where the distinct hybridization occurs between the C 2*p* and Ti 3*d* orbitals for the HOMO state. The charge density of the HOMO shown in Fig. 4(b) is indicative of a covalent bond. However, due to the electronegativity of the peripheral carbon atoms, a serious charge shifts toward the peripheral carbon atoms, denoting that the Ti–C bond is ionic. This phenomenon of charge shifting is visible in other TM–C systems as well. In order to investigate the ionic difference for various TM–C bonds, the contribution of this ionic characteristic is quantitatively described using ionicity, f_i, as suggested by Pauling [21].

$$f_i = 1 - \exp\left[-(x_A - x_B)^2/4\right] \quad (1)$$

where x_A and x_B are the electronegativities for the two interactive atoms A and B, respectively. Table 1 summarizes the calculated ionicities of the various TM–C bonds in the present work. It can be seen that the ionicity of the Ti–C bond is 0.23. Both the ionic and covalent characters are observed between the Ti and C atoms, which thus weaken the directionality of the pure covalent bond and induce the lower electron density (Fig. 2). In general, although MOs are only known to be valid when the atomic orbitals have comparable energy, the MO diagram obtained from the PDOS calculation is still reliable to extract the bond characteristics for larger energy differences. Fig. 5(b) shows the MO diagram for the Ti–C system. The HOMO is composed of hybridized C 2*p* and Ti 3*d* states, and the electrons fill all of the four bonding states as in a purely covalent bond. This resembles the previous results, in which an σ Ti–C bond was a weak, but otherwise normal, covalent bond in a serious of organotitanium compounds [22].

When the central carbon atom was replaced by V, Cr, Mn, or Fe atom, all the HOMO levels displayed the characters of nonbonding state and were composed of only the TM's 3*d* orbitals. Fig. 3(c) shows the calculation for the Cr–C system as a representative case for these TMs. The

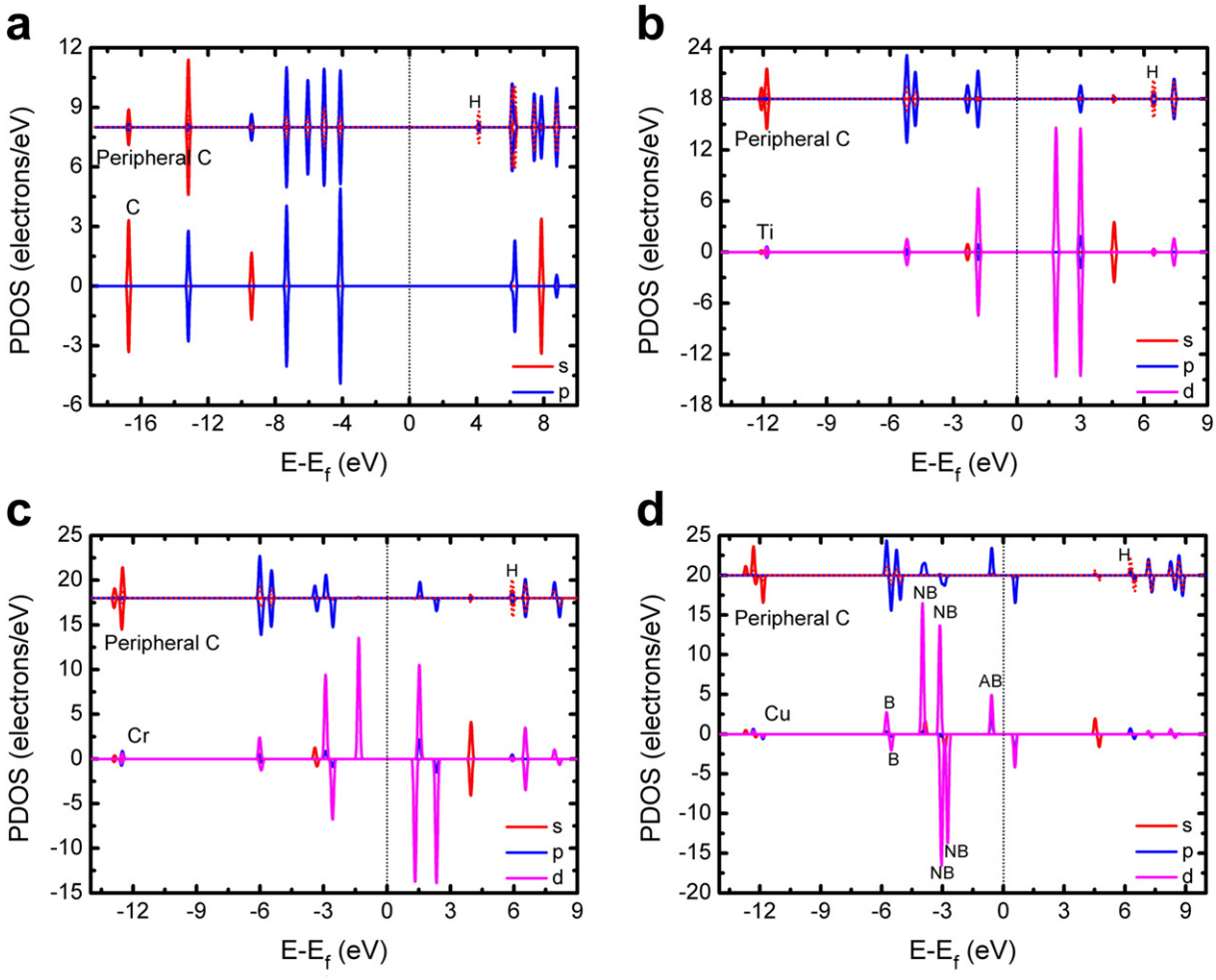

Fig. 3. PDOS projected on the central C or TM and peripheral C atoms in the (a) C–C, (b) Ti–C, (c) Cr–C, and (d) Cu–C systems, respectively.

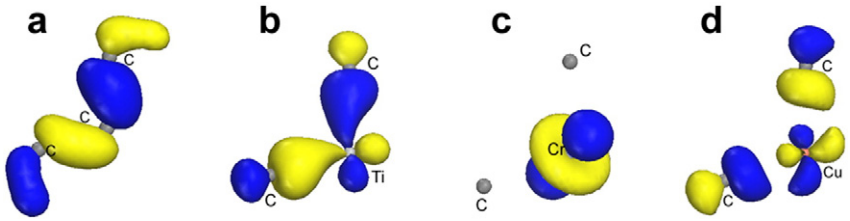

Fig. 4. The charge density between the central TM or C and peripheral C atoms for the HOMO passing through (a) C, (b) Ti, (c) Cr, or (d) Cu) and two peripheral C atoms. The blue and yellow colors indicate the positive and negative signs in the wavefunctions, respectively.

PDOS clearly indicates that only the Cr 3*d* orbital contributes to the HOMO, and no hybridization appears between the Cr 3*d* and C 2*p* orbitals. The spatial distribution of the charge density (Fig. 4(c)) also demonstrates the HOMO is isolated around the central Cr atom, revealing the nonbonding state between the Cr and C atoms in the tetrahedral system. This result is consistent with the MO diagram, as shown in Fig. 5(c), where two electrons from the Cr 3*d* are evidently located in nonbonding MO states except the four full-filled bonding states composed by C 2*p*, Cr 3*d* and Cr 4 *s* orbitals. The ionicity for this group ranges from 0.12 (Fe–C) to 0.22 (Mn–C), which is slightly less than that for Sc–C or Ti–C.

Further increasing the number of electrons in the 3*d* orbital yielded an antibonding character in the HOMO of the TM–C system. The results from the replacement of the central carbon by Co, Ni, or Cu atom demonstrated the typical antibonding characteristics. Fig. 3(d) shows that the obvious hybridization occurs between the Cu 3*d* and C 2*p* orbitals for Cu–C system, and the charge density of HOMO shown in Fig. 4(d) possesses a nodal structure with antibonding behavior between the Cu and peripheral C atoms. This unusual result implies the possibility to distort the Cu–C tetrahedron easily from its reference configuration to the lower energy state, explaining well the significant stress reduction observed from experiments. The MO diagram in Fig. 5(d) also confirms this antibonding characteristic by comparing the energy of HOMO with that of atomic states of C 2*p* and Cu 3*d*, in which three electrons occupy the antibonding states and others are to full-fill the nonbonding and bonding states with lower energy levels. Therefore, it can be said that as the number of 3*d* electrons increases to more than six, some of them will occupy the higher energy states like the antibonding state inducing the change of electron density in Fig. 2.

As noted that the residual stress of the amorphous carbon material is mainly sensitive to the deviation arising from the bond angles or bond lengths, the above bond characteristic evolution in TM-C system makes it clear beyond all doubts the discrepancy of stress reduction mechanism reported by experimental results [8–10,14–17,23]. Once the bond angles were distorted from the reference state of 109.471 to 90, 100, 120 and 130°, the resultant energy variation (ΔE) in the C–C and TM–C system could be calculated. Fig. 6 shows the ΔE for both the TM–C and pure C–C systems with various bond angles. As the 3*d* electrons of doped TM increase, the TM–C systems possess different bond

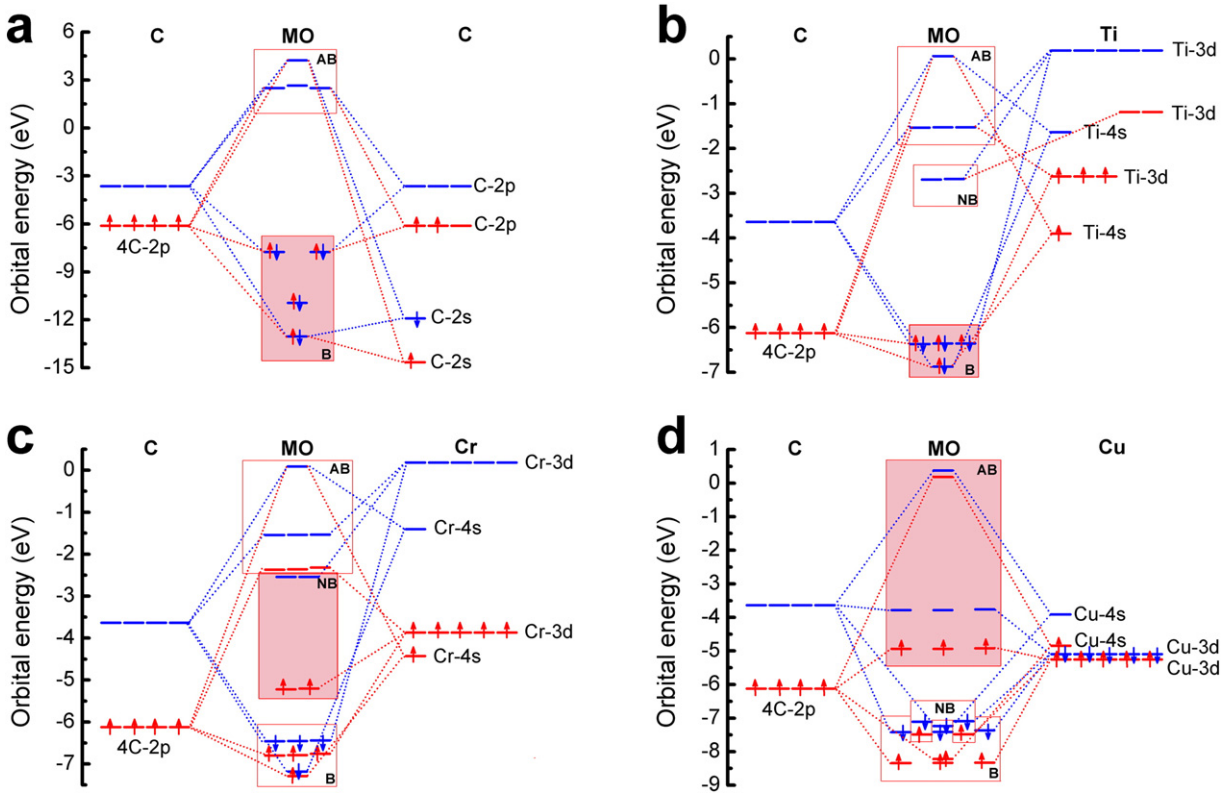

Fig. 5. MO diagrams based on the present DFT calculations with the bonding (B), nonbonding (NB) and antibonding (AB) states shown in the (a) C–C, (b) Ti–C, (c) Cr–C, and (d) Cu–C systems. The red and black arrows correspond to the spin up and spin down states, respectively.

Table 1
Calculated ionicity values when the 3*d* TM atoms bound to C.

Central atom	C	Sc	Ti	V	Cr	Mn	Fe	Co	Ni	Cu
Ionicity	0	0.30	0.23	0.19	0.18	0.22	0.12	0.11	0.10	0.10

characters, so it is observed that all of the TM–C systems possess the smaller ΔE values than that of the pure C–C unit. This originates from the ionic character between the TM and carbon atoms, which would weaken the directionality of the purely covalent bond. Therefore, the total energy of the system is less sensitive to the bond angles than that of the C–C system. In addition, since the HOMO characteristics dominate the system rigidity, it is noted that the antibonding characteristic of the HOMO for Co, Ni, and Cu drastically reduces the bond strength, which lowers the ΔE increase significantly as shown in Fig. 6.

As aforementioned, doping these 3*d* TMs into an amorphous carbon system plays the role of a pivotal site, where the distortion of bond angles can occur without the significant increase of the strain energy due to the formed bond structure in TM-doped carbon systems [9,18]. Therefore, it is supposed to be the key reason why the residual stress is generally decreased in the experimental results of TM–C system [8,9,14–17,23]. It is also expected that the doped TMs in carbon matrix would cluster because of the lower energy barrier to diffuse through the carbon network. In addition, Fig. 6 also shows that negative value of ΔE is observed at certain bond angles not only for Cu–C systems (at 90°) but also for the Co–C (at 100°) and Ni–C (at 130°) systems. This finding implies that introducing Co, Ni or Cu atoms into the carbon matrix may cause significant structural changes. Furthermore, although in this calculation only a single tetrahedral structure was considered, it is suitable to reveal the dependence of bond structure on the variety of the doped TM and clarify the pivotal action of the TM atoms in amorphous carbon matrix. The role of TM concentrations on the stress reduction in DLC films is also being further investigated by first-principles molecular dynamics simulation.

4. Conclusions

By first-principles calculation, we investigated the electronic structure of TM–C systems systematically in order to address the stress reduction mechanism that originated from the doped TMs. It is found that the atomic and electronic structure of TM–C systems strongly depends on the type of doped TM atoms, in particular, on their valence electron structure. With the doping of Sc–Cu, the bond characteristics of HOMO changed from bonding (Sc, Ti) to nonbonding (V, Cr, Mn, Fe) and finally to antibonding (Co, Ni, Cu). Furthermore, due to the different electronegativity between the doped TM and C atoms, the generated ionic characters also contributed to the HOMO. The different HOMO characters and partial ionic contributions between the TM and C atoms reduce both the strength and directionality of the formed TM–C bond, respectively. These differences account for the smaller changes of total energy upon structural distortion for TM–C system than that for pure C–C unit, demonstrating that doping a TM into an amorphous carbon matrix could decrease the residual stress of the system. The most important result in the present work is that a certain TMs such as Co, Ni, and Cu, which can form the antibonding state with widely tunable atomic structure, provide an alternative guide to fabricate the functional carbon films with high performance.

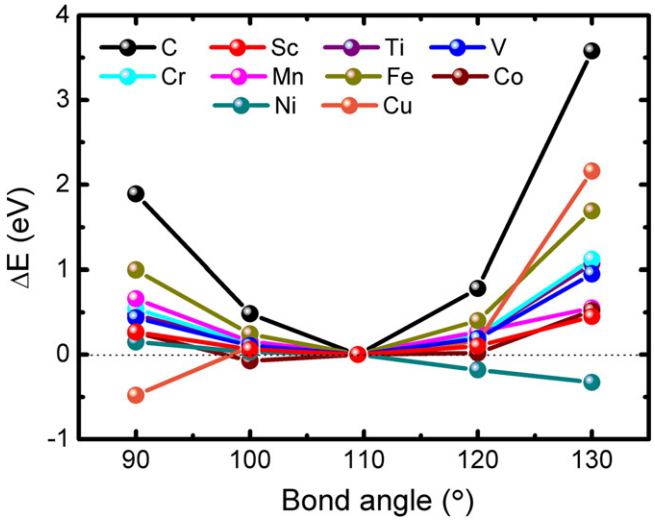

Fig. 6. Total energy changes in the TM–C and C–C systems as a function of the bond angle.

Acknowledgments

This research was supported by the National Natural Science Foundation of China (51402319, 51522106), International Cooperation Foundation of Ningbo government (2015D10004) and Ningbo Municipal Natural Science Foundation (2015A610089). The authors thank Prof. Liang Chen at Ningbo Institute of Materials Technology and Engineering, Chinese Academy of Sciences, for providing the supercomputer platform and productive discussion.

References

[1] J. Robertson, Hard amorphous (diamond-like) carbons, Prog. Solid State Chem. 21 (1991) 199–333.
[2] N. Dwivedi, S. Kumar, J.D. Carey, R.K. Tripathi, H.K. Malik, M.K. Dalai, Influence of silver incorporation on the structural and electrical properties of diamond-like carbon thin films, ACS Appl. Mater. Interfaces 5 (2013) 2725–2732.
[3] J. Wang, J. Pu, G. Zhang, L. Wang, Interface architecture for superthick carbon-based films toward low internal stress and ultrahigh load-bearing capacity, ACS Appl. Mater. Interfaces 5 (2013) 5015–5024.
[4] Z.D. Sha, V. Sorkin, P.S. Branicio, Q.X. Pei, Y.W. Zhang, D.J. Srolovitz, Large-scale molecular dynamics simulations of wear in diamond-like carbon at the nanoscale, Appl. Phys. Lett. 103 (2013) 073118.
[5] A.H. Lettington, Applications of diamond-like carbon thin films, Carbon 36 (1998) 555–560.
[6] C. Casiraghi, J. Robertson, A.C. Ferrari, Diamond-like carbon for data and beer storage, Mater. Today 10 (2007) 44–53.
[7] N. Konofaos, C.B. Thomas, Characterization of heterojunction devices constructed by amorphous diamondlike films on silicon, J. Appl. Phys. 81 (1997) 6238–6245.
[8] W. Dai, P. Ke, M.W. Moon, K.R. Lee, A. Wang, Investigation of the microstructure, mechanical properties and tribological behaviors of Ti-containing diamond-like carbon films fabricated by a hybrid ion beam method, Thin Solid Films 520 (2012) 6057–6063.
[9] A.Y. Wang, H.S. Ahn, K.R. Lee, J.P. Ahn, Unusual stress behavior in W-incorporated hydrogenated amorphous carbon films, Appl. Phys. Lett. 86 (2005) 111902.
[10] Y.T. Pei, C.Q. Chen, K.P. Shaha, J.Th.M. De Hosson, J.W. Bradley, S.A. Voronin, M. Čada, Microstructural control of TiC/a-C nanocomposite coatings with pulsed magnetron sputtering, Acta Mater. 56 (2008) 696–709.
[11] X. Liao, X. Zhang, K. Takai, T. Enoki, Electric field induced sp^3-to-sp^2 conversion and nonlinear electron transport in iron-doped diamond-like carbon thin film, J. Appl. Phys. 107 (2010) 013709.
[12] N. Menegazzo, C. Jin, R.J. Narayan, B. Mizaikoff, Compositional and electrochemical characterization of noble metal-diamondlike carbon nanocomposite thin films, Langmuir 23 (2007) 6812–6818.
[13] J.A. Colón Santana, R. Skomski, V. Singh, V. Palshin, A. Petukhov, Ya.B. Losovy, A. Sokolov, P.A. Dowben, I. Ketsman, Magnetism of Cr-doped diamond-like carbon, J. Appl. Phys. 105 (2009) 07A930.
[14] A.Y. Wang, K.R. Lee, J.P. Ahn, J.H. Han, Structure and mechanical properties of W incorporated diamond-like carbon films prepared by a hybrid ion beam deposition technique, Carbon 44 (2006) 1826–1832.
[15] J. Musil, M. Louda, Z. Soukup, M. Kubásek, Relationship between mechanical properties and coefficient of friction of sputtered a-C/Cu composite thin films, Diam. Relat. Mater. 17 (2008) 1905–1911.
[16] H.W. Choi, J.H. Choi, K.R. Lee, J.P. Ahn, K.H. Oh, Structure and mechanical properties of Ag-incorporated DLC films prepared by a hybrid ion beam deposition system, Thin Solid Films 516 (2007) 248–251.
[17] N.K. Manninen, F. Ribeiro, A. Escudeiro, T. Polcar, S. Carvalho, A. Cavaleiro, Influence of Ag content on mechanical and tribological behavior of DLC coatings, Surf. Coat. Technol. 232 (2013) 440–446.
[18] J.H. Choi, S.C. Lee, K.R. Lee, A first-principles study on the bond characteristics in carbon containing Mo, Ag, or Al impurity atoms, Carbon 46 (2008) 185–188.

[19] X. Li, P. Ke, H. Zheng, A. Wang, Structural properties and growth evolution of diamond-like carbon films with different incident energies: a molecular dynamics study, Appl. Surf. Sci. 273 (2013) 670–675.
[20] J.P. Perdew, K. Burke, M. Ernzerhof, Generalized gradient approximation made simple, Phys. Rev. Lett. 77 (1996) 3865–3868.
[21] L. Pauling, The Nature of the Chemical Bond, third ed. Cornell University Press, New York, 1960.
[22] J.A. Waters, G.A. Mortimer, Synthesis and some characteristics of di-π-cyclopentadienyl-σ-organotitanium (IV) chlorides, J. Organomet. Chem. 22 (1970) 417–424.
[23] W. Dai, A. Wang, Q. Wang, Microstructure and mechanical property of diamond-like carbon films with ductile copper incorporation, Surf. Coat. Technol. 272 (2015) 33–38.